2017

Highly porous photoluminescent diazaborole-linked polymers: synthesis, characterization, and application to selective gas adsorption

Zafer Kahveci
Virginia Commonwealth University

Ali K. Sekizkardes
Virginia Commonwealth University

Ravi K. Arvapally
Virginia Commonwealth University

Logan Wilder
Virginia Commonwealth University

Hani M. El-Kaderi
Virginia Commonwealth University

Polymer Chemistry

PAPER

View Article Online
View Journal | View Issue

Cite this: *Polym. Chem.*, 2017, **8**, 2509

Highly porous photoluminescent diazaborole-linked polymers: synthesis, characterization, and application to selective gas adsorption†

Zafer Kahveci, Ali K. Sekizkardes, Ravi K. Arvapally, Logan Wilder and Hani M. El-Kaderi*

Received 14th December 2016,
Accepted 27th March 2017

DOI: 10.1039/c6py02156e

rsc.li/polymers

The formation of boron–nitrogen (B–N) bonds has been widely explored for the synthesis of small molecules, oligomers, or linear polymers; however, its use in constructing porous organic frameworks remains very scarce. In this study, three highly porous diazaborole-linked polymers (DBLPs) have been synthesized by condensation reactions using 2,3,6,7,14,15-hexaaminotriptycene and aryl boronic acids. DBLPs are microporous and exhibit high Brunauer–Emmett–Teller surface area (730–986 $m^2\ g^{-1}$) which enable their use in small gas storage and separation. At ambient pressure, the amorphous polymers show high CO_2 (DBLP-4: 4.5 mmol g^{-1} at 273 K) and H_2 (DBLP-3: 2.13 wt% at 77 K) uptake while their physicochemical nature leads to high CO_2/N_2 (35–42) and moderate CO_2/CH_4 (4.9–6.2) selectivity. The electronic impact of integrating diazaborole moieties into the backbone of these polymers was investigated for DBLP-4 which exhibits green emission with a broad peak ranging from 350 to 680 nm upon excitation with 340 nm in DMF without photobleaching. This study demonstrates the effectiveness of B–N formation in targeting highly porous frameworks with promising optical properties.

1. Introduction

Porous organic polymers (POPs) have attracted significant attention in recent years due to their potential in gas storage and separation, conductivity, catalysis, electronics, and chemical sensing.[1–6] POPs are synthesized using versatile synthetic routes while their chemical composition and textural properties can be tailored to optimize their multifaceted uses. During synthesis, the covalent nature of POPs renders them amorphous unless thermodynamic and kinetic parameters are controlled as in the case of covalent organic frameworks (COFs) which form microcrystalline materials wherein the building units linked by B–O, C–N, and B–N bonds.[7–11] Amorphous POPs prepared from the formation of these bonds and C–C bonds are documented in literature and they include PAFs,[12] triazine-based polyimides (TPIs),[13] triptycene-based polymers of intrinsic microporosity (Trip(Et)-PIM),[14] polycarbazoles (CPOPs)[15] imine-linked microporous polymers,[16,17] azo-linked polymers (ALPs),[18] and benzimidazole-linked polymers (BILPs).[19–23] Surprisingly and in spite of the growing interest in this area, there are only very few examples of porous networks preparation through B–N bond formation, namely, borazine-linked polymers (BLPs)[24–27] and B,N-containing cross-linked polymers (PPs-BN).[28] We have demonstrated that the formation of borazine (B_3N_3, Fig. 1B) which is analogous to boroxine (B_3O_3, Fig. 1A) in COFs can lead to porous frameworks that show good thermal stability and interesting gas

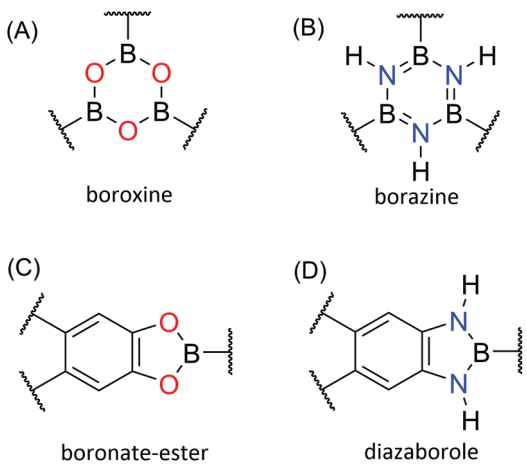

Fig. 1 Boroxine (A) and boronate-ester (C) building blocks and their borazine (B) and diazaborole analogs.

Department of Chemistry, Virginia Commonwealth University, Richmond, Virginia 23284-2006, USA. E-mail: helkaderi@vcu.edu

†Electronic supplementary information (ESI) available: Spectral and physical characterization of diazaborole-linked polymers and their gas uptake and selectivity studies. See DOI: 10.1039/c6py02156e

uptake properties.[24–27] Another effective method for boron incorporation into COFs is through condensation reactions that lead to boronate-ester linkage formation (C_2O_2B, Fig. 1C). To expand on the use of B–N bond in constructing porous networks we envisioned that the formation of diazaborole (C_2N_2B, Fig. 1D) would lead to new porous networks for potential use in gas storage and optical applications. Although 5-membered diazaborole rings have been used to modify the photophysical properties of linear polymers as well as small molecules,[29–32] their use in porous networks remains unprecedented to the best of our knowledge.

In this study, we report the first use of B–N bond formation to construct highly porous diazaborole-linked polymers (DBLPs) and investigate their porosity and application in small gas storage. DBLPs are highly porous and show high CO_2 and H_2 uptake, high CO_2 selectivity over N_2 and CH_4 as well as high thermal stability.

2. Experimental methods

All starting materials, unless noted otherwise, were obtained from Acros Organics and used without further purification. 1,2,4,5-Benzenetetramine tetrahydrochloride (BTA), triptycene, chloroform (stabilized with amylene) and *N*-*N*-dimethylformamide (DMF) were purchased from Aldrich Chemical Co. and used without further purification. Solvents were dried by distillation from Na (toluene) or Na/benzophenone (THF). 1,3,5-benzenetriboronic acid (BTBA)[33,34] and 2,3,6,7,14,15-hexaaminotriptycene (HATT)[20] were synthesized according to published methods. All products were handled under nitrogen atmosphere using glovebox or Schlenk line techniques. Solution ^{1}H NMR spectra were taken by Varian Mercury-300 MHz NMR spectrometer (75 MHz carbon frequency). Solid-state ^{13}C cross-polarization magic angle spinning (CP-MAS) NMR spectra of solid samples were obtained by Spectral Data Services, Inc. Spectra were obtained using Tecmag-based NMR spectrometer, operated at a H-1 frequency of 363 MHz, using contact time of 1 ms and delay of three seconds for CP-MAS experiments. Thermogravimetric analysis (TGA) was carried out by a TA Instruments Q-5000IR series thermal gravimetric analyzer using 50 μL platinum pans under flow of N_2 gas with heating rate of 5 °C min^{-1}. To obtain Scanning Electron Microscopy (SEM) images, each sample was dispersed onto a sticky carbon surface attached to a flat aluminum sample holder. Then, the sample was coated with platinum at pressure of 1×10^{-5} mbar in nitrogen atmosphere for 90 seconds before imaging. SEM images were taken by a Hitachi SU-70 Scanning Electron Microscope. Powder X-ray diffraction patterns were collected on a Panalytical X'pert pro multipurpose diffractometer (MPD) with Cu Kα radiation. FT-IR spectra were obtained by a Nicolet-Nexus 670 spectrometer having an attenuated total reflectance accessory. Porosity and gas sorption experiments were carried out using a Quantachrome Autosorb iQ volumetric analyzer using UHP grade adsorbates. All samples were degassed at 120 °C under vacuum before gas sorption measurements. Pore Size Distribution (PSD) was calculated from Ar isotherms using spherical/cylindrical pore (zeolite) NLDFT adsorption branch model.

2.1 Preparation of DBLP-3

1,4-Benzenediboronic acid (BDBA) (42 mg, 0.25 mmol) and 2,3,6,7,14,15-hexaaminotriptycene (HATT) (100 mg, 0.18 mmol) were grained into a mortar and suspended in 30 mL of dry *N*-*N*-dimethylformamide (DMF) under a nitrogen atmosphere in a 100 mL Schlenk flask. After 10 minutes bubbling nitrogen gas, the mixture was sonicated for 30 minutes. The flask was transferred into an oven and gradually heated until 130 °C then kept at that temperature for three days. Then the flask was taken into glovebox, filtered over medium glass frit and washed with dry DMF and dry acetone. The product was soaked in dry acetone/DMF (50 : 50 v : v) mixture for 12 hours at which point the solvent was decanted and only dry acetone was added for 12 hours more. Decantation and addition of fresh acetone was repeated once more. The solid was then filtrated and activated at 120 °C under reduced pressure for 16 hours to afford DBLP-3 (53 mg, 65% yield) as a greenish solid. Anal. Calcd for $C_{58}H_{34}B_6N_{12}$: C, 71.83%; H, 4.16%; N, 17.33%; Found: C, 59.82%; H, 4.19%; N, 12.53%.

2.2 Preparation of DBLP-4

This polymer was synthesized following the methods mentioned above for DBLP-3 using 1,3,5-benzenetris (4-phenylboronic acid) (BTPA) (46.6 mg, 0.094 mmol) and 2,3,6,7,14,15-hexaaminotriptycene (HATT) (60 mg, 0.107 mmol). After drying, the final product DBLP-4 was obtained as off-white solid (42 mg, 66% yield). Anal. Calcd for $C_{44}H_{29}B_3N_6$: C, 78.39%; H, 4.34%; N, 12.47%. Found: C, 70.22%; H, 4.99%; N, 8.52%.

2.3 Preparation of DBLP-5

This polymer was synthesized following the methods mentioned above for DBLP-3 using tetra(4-dihydroxyborylphenyl) methane (TBPM) (40 mg, 0.080 mmol) and 2,3,6,7,14,15-hexaaminotriptycene (HATT) (60 mg, 0.107 mmol). After drying, the final product DBLP-5 was obtained as off-white solid (58 mg, 60% yield). Anal. Calcd for $C_{155}H_{104}B_{12}N_{24}$: C, 76.54%; H, 4.31%; N, 13.82%. Found: C, 66.79%; H, 4.72%; N, 8.14%.

Note: Organoboron compounds typically give lowered carbon and nitrogen values in elemental microanalysis due to the formation of non-combustible boron carbide and boron nitride byproducts.[24–27]

3. Results and discussion

3.1 Synthesis and characterization of DBLPs

The synthesis of all DBLPs was carried out by condensation reactions between aryl boronic acids and 2,3,6,7,14,15-hexaaminotriptycene (HCl salt) in anhydrous DMF under nitrogen atmosphere at 130 °C for 3 days as shown in Scheme 1. All

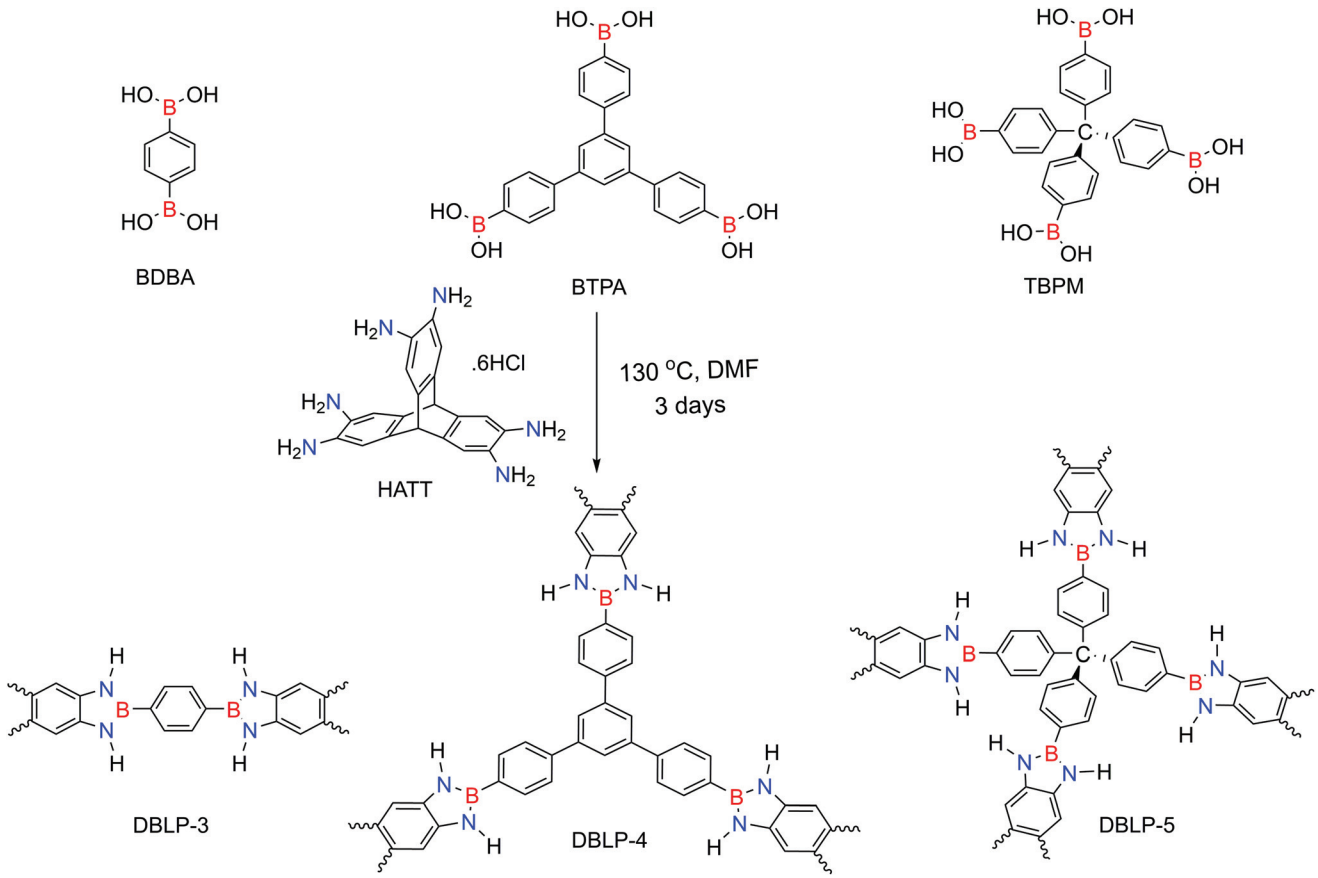

Scheme 1 Synthesis of triptycene-derived diazaborole-linked polymers (DBLPs).

polymers were purified by soaking in THF and acetone to solubilize and remove the unreacted boronic acid and amine containing starting materials. Subsequently, polymers were prepared for the spectral, analytical and porosity measurements by drying under reduced pressure and heating at 120 °C. The chemical composition, stability, and phase purity and the amorphous nature of the DBLPs were established using elemental analysis, FT-IR, solid-state ^{11}B and ^{13}C CP-MAS, SEM and XRD, as well as porosity measurements. Scanning electron microscopy (SEM) of the polymers revealed aggregated fine particles of variable size in the range of ~0.4 to 1.0 μm (Fig. S1 ESI†). Thermogravimetric analysis (TGA) showed initial weight loss up to around 100 °C which corresponds to the removal of adsorbed moisture or residual solvents in the pores then decomposition starts around 350 °C (Fig. S2 ESI†). The FT-IR spectrum of DBLPs (Fig. S3 ESI†) revealed N–H stretching at around 3400 cm^{-1} (free N–H) and disappearance of broad O–H vibrations of boronic acid units, while intense new bands appeared at 1423 cm^{-1} (B–N, double bond character), 1171 cm^{-1} (B–N, single bond character), and 1012 cm^{-1} (B–C stretch) that can be assigned to skeleton vibration of the diazaborole ring.[32,35–37] The solid-state ^{11}B (Fig. S4 ESI†) revealed a broad signal ranging from 19.8 ppm to 8.0 ppm which falls in the reported tri-coordinate boron atoms[38] and the ^{13}C CP-MAS studies (Fig. S4 ESI†) further support the incorporation of the triptycene and aryl moieties from the boronic acids into the framework of DBLPs.

3.2 Optical properties

The impact of copolymerization can also be easily noted from the photophysical properties of DBLPs; we selected one of the polymers, DBLP-4, for UV-Vis studies and compared the results to those of the building units as well as the covalent organic framework that could form upon self-condensation of 1,3,5-tris [4-phenylboronicacid] benzene. Upon exciting DBLP-4 with 340 nm in DMF, green emission with broad peak ranging from 350 to 680 nm is observed (Fig. 2). Compared to both triptycene and the triphenyl boronic acid, the excitation peak of DBLP-4 exhibits a bathochromic shift (Fig. 2). Similarly, the emission peak in DBLP-4 shows a red shift. The red shift in both excitation and emission indicates an increased conjugation due to the formation of diazaborole link involving one of the benzene rings from triptycene and the boron part of the triphenyl boronic acid. It is worth noting that DBLP-4 is stable to light and did not exhibit any degradation as the sample was exposed to UV light for 40 minutes according to photobleaching studies (Fig. S5 ESI†). For comparison, the UV-Vis results for DBLP-3 and DBLP-5 are depicted in Fig. S5 ESI.† Similar photophysical properties results have been reported for nonporous sidechain diazaborole

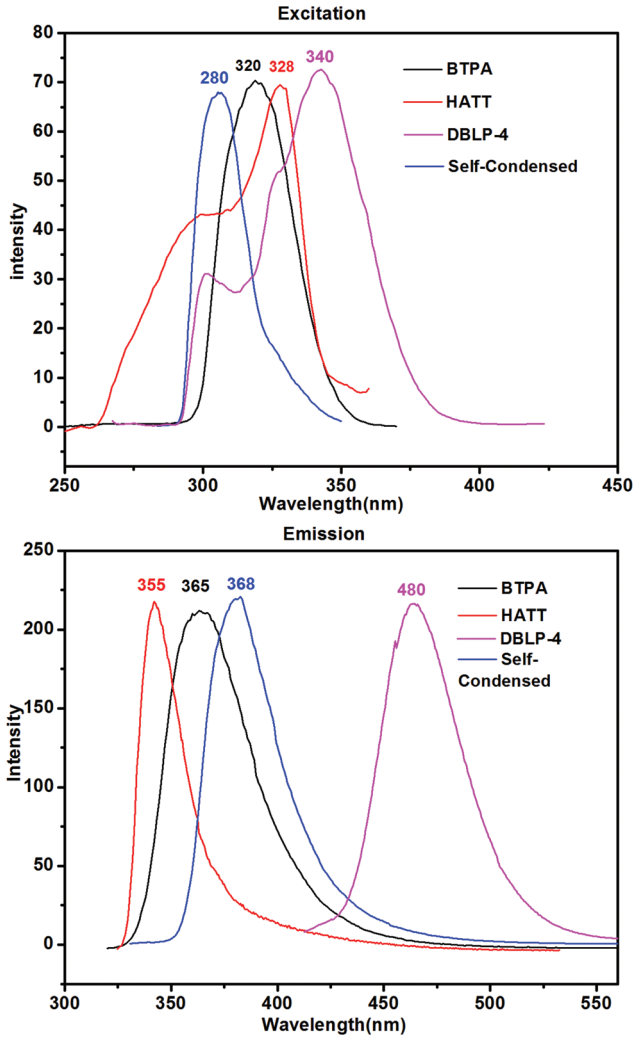

Fig. 2 Excitation and Emission spectra of BTPA, HATT, DBLP-4 and self-condensed BTPA in DMF.

functionalized linear polymers or oligomers linked by diazaborole units.[29–32] Compared to DBLP-3 and DBLP-5, the emission spectrum of DBLP-4 is red shifted (Fig. S6 ESI†). This is due to the differences in the structural arrangement of these three different polymers. DBLP-3 has one benzene ring as the central core, DBLP-5 has four benzene rings connected by carbon atom at the central core whereas DBLP-4 has one triphenyl benzene which is highly conjugated. The higher the conjugation the longer the emission wavelength. As these polymers are emissive and have boron atom which is electron deficient, they would be useful for sensing anions such as halides.

3.3 Porosity and gas uptake studies

To investigate the porous nature of DBLPs, we performed Ar porosity measurements at 87 K (Fig. S8 ESI†). Samples of purified polymers were degassed at 120 °C for 12 h under 1×10^{-5} Torr vacuum to remove any adsorbed gases or moisture before sorption measurements. The fully reversible type I–IV isotherms show a rapid uptake at low pressure (P/P_0 = 0 to 0.05 bar) and are indicative of microporosity. A minor hysteresis for all samples is consistent with their powdery and flexible nature of organic polymers. Applying the Brunauer–Emmett–Teller (BET) model to the sorption branch within the pressure range of P/P_0 = 0.05–0.15 resulted in surface areas of 730 $m^2 g^{-1}$ (DBLP-3), 904 $m^2 g^{-1}$ (DBLP-4), and 986 $m^2 g^{-1}$ (DBLP-5). We have recently reported the use of the triptycene building unit in the synthesis of several classes of porous organic polymers; COFs,[39] azo-linked polymers (ALPs)[18] and benzimidazole-linked polymers (BILPs).[20,21] Triptycene is well known for enhancing the porosity of polymers of intrinsic microporosity (PIMs),[14] shape-persistent case molecules,[40] metal salphens,[41] and MOFs.[42] It possesses high degree of internal molecular free volume (IMFV).[43,44] Pore size distribution (PSD) studies using nonlocal density functional theory (NLDFT) (Fig. S9 and 10 ESI†) were used to evaluate the potential impact of network interpenetration and cross-linking on the porosity level of DBLPs. Argon isotherms were fitted with NLDFT and PSD were found to be centered around 6.6, 6.7, and 7.4 Å, while the pore volume was calculated from single point measurements (P/P_0 = 0.95) and found to be 0.5, 0.52, and 0.68 cc g^{-1} for DBLP-3, DBLP-4, and DBLP-5, respectively. The results from PSD studies revealed that the structures of the DBLPs are most likely disordered and highly interpenetrated compared to crystalline COF structures derived from the analogous boronate-ester linkage. For instance, TDCOF-5[39] which is analogous to DBLP-3 has much larger pores (26 Å) and surface area (SA_{BET} = 2497). These results indicate that the polymerization processes which lead to B–N bond formation in DBLPs seem to have little control over pore metrics. This was not surprising giving the less labile nature of B–N when compared to B–O bonds.[45–47]

All DBLPs have sub-nanometer pores rich in heteroatoms (C, N, H, and B) which are attractive features for the study of small gas storage and separation applications. Accordingly, gas uptake measurements were collected for H_2, CO_2, and CH_4 at low pressure (1.0 bar) as shown in Fig. 3. The CO_2 gas adsorption performance of DBLPs is depicted in Fig. 3A. The CO_2 isotherms collected at 273 K up to 1 bar are fully reversible and exhibit a steep rise at low pressures. The CO_2 sorption of the DBLP-4 found to be 198 mg g^{-1} (4.50 mmol g^{-1}) at 273 K and 1 bar which is higher than BLPs (74–128 mg g^{-1}),[24–26] BILP-10 (177 mg g^{-1}),[19] and also wide range of porous organic polymers such as and –OH functionalized porous organic frameworks (POFs: 4.2 mmol g^{-1}),[48] functionalized CMPs (1.6–1.8 mmol g^{-1}),[49] and triptycene-based microporous poly(benzimidazole) networks TBIs (2.7–3.9 mmol g^{-1}).[50] The CO_2 uptake of DBLP-4 is also similar with those of the best performing organic polymers such as BILP-7/4 (4.5/5.3 mmol g^{-1}).[21]

In addition to CO_2 capture, hydrogen storage studies have been considered due to their potential use in automotive applications and their abundance and clean aspects. The hydrogen uptake by DBLPs (1.73–2.13 wt%) at 77 K and 1 bar (Fig. 3B) are higher than most of the microporous organic

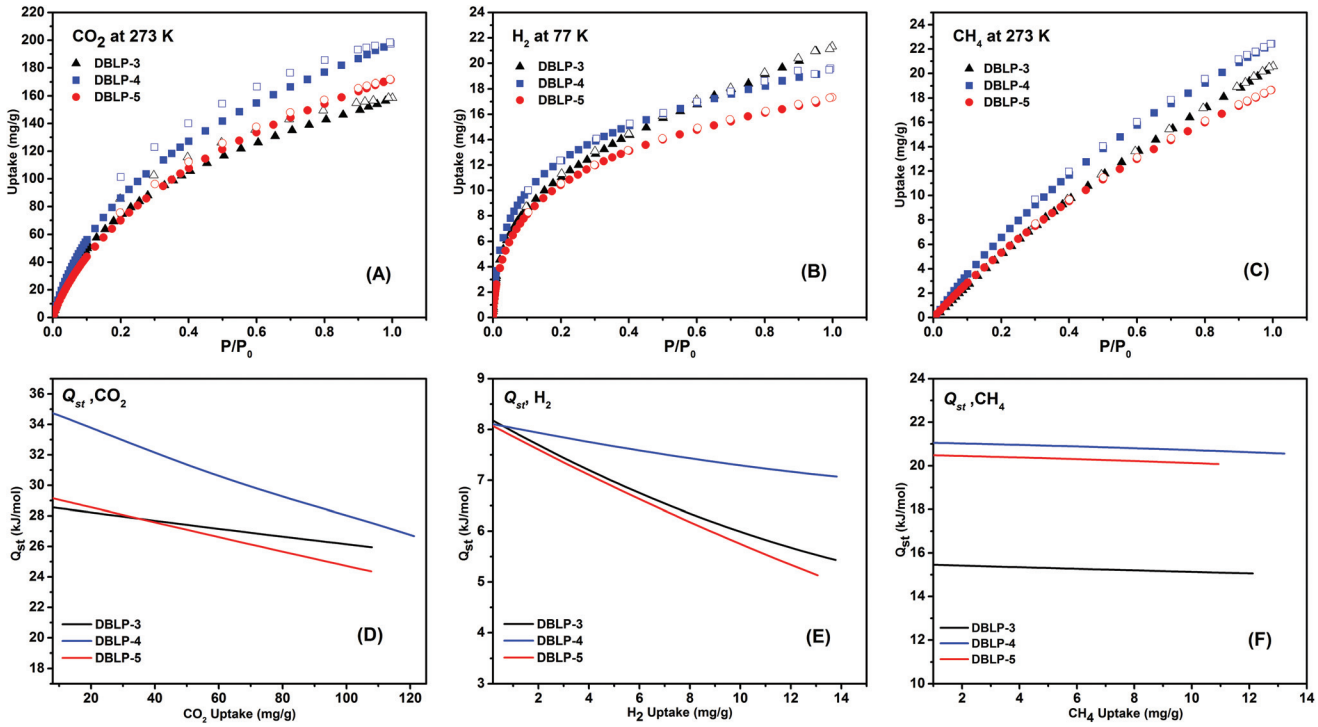

Fig. 3 Gas uptake isotherms: CO_2 (A), H_2 (B), CH_4 (C), and Q_{st} CO_2 (D), H_2(E), and CH_4 (F).

polymers.[14,51] Additionally, CH_4 uptakes were in the range of 18.7–22.4 mg g^{-1}. The binding affinity of CO_2, CH_4 and H_2 was calculated from sorption data collected at 273 K and 298 K by using the virial method. DBLPs exhibited high heats of adsorption (Q_{st}) for CO_2 ranging from 28.6 to 35.3 kJ mol^{-1} at low coverage (Fig. 3D and S13 ESI†). Similar Q_{st} ranges have been also reported for several porous materials that show high CO_2 capturing capacity such as BILPs (26.7–28.8 kJ mol^{-1}),[19–21,52] PECONFs (26–34 mol^{-1})[53] or PI-1 (34 mol^{-1}).[54] The high Q_{st} values can be attributed to their narrow pores that facilitate CO_2-multiwall interactions and the formation of CO_2···H–N hydrogen bonding.[32] Noteworthy, it was reported that the N–H sites of diazaborole form hydrogen bonds by intramolecular interactions with oxygen atoms of neighboring quinine units characterized by short C═O···H–N bonds (2.09 Å). Therefore, it is most likely that the high bonding affinity and CO_2 uptake by DBLPs would benefit from similar interactions.[32] A small depletion in Q_{st} at higher CO_2 loading suggests saturation of favorable CO_2 binding sites of DBLPs that become less accessible with increasing CO_2 pressure.[23,55] In a similar way, hydrogen Q_{st} values were calculated at zero-coverage, the Q_{st} values for DBLPs are around 8.1 kJ mol^{-1} (Fig. 3E and S14 ESI†). The Q_{st} values are higher than the values reported for organic polymers such as polyimide networks (5.3–7.0 kJ mol^{-1}),[56–58] porous aromatic frameworks (PAF-1, 4.6 kJ mol^{-1}),[59] porous polymer networks (PPNs, 5.5–7.6 kJ mol^{-1}),[60] and comparable with BILPs (7.8–8.3 kJ mol^{-1}),[19–21,52] and –OH functionalized POFs (8.3 kJ mol^{-1}).[61] Unlike the CO_2 uptake, decoration of framework with polar groups does not enhance the methane uptake[62] as a result of non-polar nature of the methane which is evidenced by relatively low enthalpies of adsorption (15.5 to 21.1 kJ mol^{-1}) (Fig. S15 ESI†). Although, framework interaction with methane is weaker than CO_2, yet still strong enough to accommodate high methane uptake at low pressures and inline with most porous materials in the field.[58,62–64]

There have been great efforts to design an adsorbent which is selectively capture the targeted gas molecule. CO_2 is not the main component in gas mixtures, and selective CO_2 removal from mixtures such as flue gas (~75% nitrogen) is needed in addition to high capacity for CO_2. Therefore, CO_2/N_2 and CO_2/CH_4 selectivity has been calculated for flue gas and landfill gas, respectively, using Henry's law initial slope selectivity calculations which generally give decent assessment for selectivity were applied to single-component gas adsorption isotherms obtained at 273 K and 298 K (Fig. 4 and S16, 17 ESI†) as summarized in Table 1. Recent selectivity studies of several porous adsorbents demonstrated that high CO_2 uptake coupled with narrow pore size are advantageous for selective CO_2 capture.[65–67] Following this trend, DBLP-4 showed higher CO_2/N_2 selectivity (51) at 298 K compared to DBILP-3 (42) and DBLP-5 (35) as shown in Table 1 due to the high Q_{st} value of DBLP-4. In general, polymers with high Q_{st} for CO_2 result in higher CO_2 selectivity,[55] because they exhibit high CO_2 uptake at low pressures. Overall, all DBLPs showed high selectivity for CO_2/N_2 (35–51) at 298 K which is comparable with those of BILPs,[19–21,52] MOPs,[55] COPs,[68] NPOFs,[69] and ALPs.[18] Moreover, the CO_2/CH_4 selectivity values for all polymers fall in the range of 4.9 to 6.2.

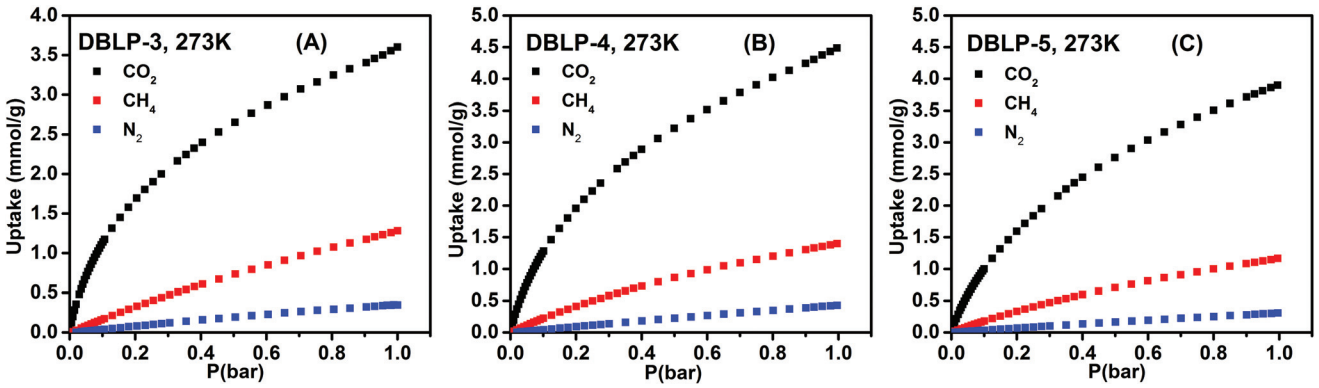

Fig. 4 CO_2, CH_4, and N_2 gas uptake isotherms at 273 K of DBLPs.

Table 1 Gas uptake and selectivity (CO_2/N_2 and CO_2/CH_4) for DBLPs

		H_2 at 1 bar[b]			CO_2 at 1 bar[b]			CH_4 at 1 bar[b]			N_2 at 1 bar[b]		Selectivity[c]	
Polymer	SA_{BET}/SA_{Lang}[a]	77 K	87 K	Q_{st}	273 K	298 K	Q_{st}	273 K	298 K	Q_{st}	273 K	298 K	CO_2/N_2	CO_2/CH_4
DBLP-3	730/893	21.3	14.4	8.1	158.5	108	28.6	20.6	12.2	15.5	16.6	3.8	42	6.2
DBLP-4	904/1040	19.6	13.8	8.1	198	173	35.3	22.4	13.2	21.1	12.0	2.8	51	4.9
DBLP-5	986/1143	17.3	13.0	8.1	171.5	108	29.5	18.7	10.9	20.5	8.6	3.9	35	5.9

[a] Surface area ($m^2\ g^{-1}$) was calculated from Ar isotherm. [b] Gas uptake in mg g^{-1} and the isosteric enthalpies of adsorption (Q_{st}) in kJ mol^{-1}. [c] Selectivity (mol mol^{-1}) was calculated from initial slope calculations at 298 K.

4. Conclusions

To conclude, we have successfully synthesized and characterized a new class of porous polymer, named DBLPs and investigated their potential in small gas uptake and separation. DBLPs can be synthesized through condensation reactions between boronic acid building blocks and orthodiamine-containing monomers with high surface area and sub-nanometer pore size. These polymers exhibit remarkable CO_2 uptake (up to 4.5 mmol g^{-1}) and good CO_2 selectivity over N_2 that can reach up to 51 at 1 bar and 298 K. In addition to high CO_2 uptake and selectivity, DBLPs show interesting optical properties which could open the door for other applications.

Acknowledgements

Research supported by the U.S. Department of Energy, Office of Basic Energy Sciences, Division of Materials Sciences and Engineering under award number DE-SC0002576.

References

1 D. Wu, F. Xu, B. Sun, R. Fu, H. He and K. Matyjaszewski, *Chem. Rev.*, 2012, **112**, 3959–4015.
2 Y. Zhang and S. N. Riduan, *Chem. Soc. Rev.*, 2012, **41**, 2083–2094.
3 P. Kaur, J. T. Hupp and S. T. Nguyen, *ACS Catal.*, 2011, **1**, 819–835.
4 S. Das, P. Heasman, T. Ben and S. Qiu, *Chem. Rev.*, 2017, **117**, 1515–1563.
5 A. G. Slater and A. I. Cooper, *Science*, 2015, **348**, 988–998.
6 R. Dawson, A. I. Cooper and D. J. Adams, *Prog. Polym. Sci.*, 2012, **37**, 530–563.
7 H. M. El-Kaderi, J. R. Hunt, J. L. Mendoza-Cortés, A. P. Côté, R. E. Taylor, M. O'Keeffe and O. M. Yaghi, *Science*, 2007, **316**, 268–272.
8 C. S. Diercks and O. M. Yaghi, *Science*, 2017, **355**, 923–931.
9 P. J. Waller, F. Gándara and O. M. Yaghi, *Acc. Chem. Res.*, 2015, **48**, 3053–3063.
10 S.-Y. Ding and W. Wang, *Chem. Soc. Rev.*, 2013, **42**, 548–568.
11 X. Feng, X. Ding and D. Jiang, *Chem. Soc. Rev.*, 2012, **41**, 6010–6022.
12 T. Ben and S. Qiu, *CrystEngComm*, 2013, **15**, 17–26.
13 M. R. Liebl and J. Senker, *Chem. Mater.*, 2013, **25**, 970–980.
14 B. S. Ghanem, M. Hashem, K. D. M. Harris, K. J. Msayib, M. Xu, P. M. Budd, N. Chaukura, D. Book, S. Tedds, A. Walton and N. B. McKeown, *Macromolecules*, 2010, **43**, 5287–5294.
15 Q. Chen, M. Luo, P. Hammershøj, D. Zhou, Y. Han, B. W. Laursen, C.-G. Yan and B.-H. Han, *J. Am. Chem. Soc.*, 2012, **134**, 6084–6087.
16 M. G. Rabbani, A. K. Sekizkardes, Z. Kahveci, T. E. Reich, R. Ding and H. M. El-Kaderi, *Chem. – Eur. J.*, 2013, **19**, 3324–3328.
17 P. Pandey, A. P. Katsoulidis, I. Eryazici, Y. Wu, M. G. Kanatzidis and S. B. T. Nguyen, *Chem. Mater.*, 2010, **22**, 4974–4979.

18 P. Arab, M. G. Rabbani, A. K. Sekizkardes, T. Islamoglu and H. M. El-Kaderi, *Chem. Mater.*, 2014, **26**, 1385–1392.
19 M. G. Rabbani, A. K. Sekizkardes, O. M. El-Kadri, B. R. Kaafarani and H. M. El-Kaderi, *J. Mater. Chem.*, 2012, **22**, 25409–25417.
20 M. G. Rabbani, T. E. Reich, R. M. Kassab, K. T. Jackson and H. M. El-Kaderi, *Chem. Commun.*, 2012, **48**, 1141–1143.
21 M. G. Rabbani and H. M. El-Kaderi, *Chem. Mater.*, 2012, **24**, 1511–1517.
22 M. G. Rabbani and H. M. El-Kaderi, *Chem. Mater.*, 2011, **23**, 1650–1653.
23 S. Altarawneh, S. Behera, P. Jena and H. M. El-Kaderi, *Chem. Commun.*, 2014, 3571–3574.
24 K. T. Jackson, M. G. Rabbani, T. E. Reich and H. M. El-Kaderi, *Polym. Chem.*, 2011, **2**, 2775–2777.
25 K. T. Jackson, T. E. Reich and H. M. El-Kaderi, *Chem. Commun.*, 2012, **48**, 8823–8825.
26 T. E. Reich, S. Behera, K. T. Jackson, P. Jena and H. M. El-Kaderi, *J. Mater. Chem.*, 2012, **22**, 13524–13528.
27 T. E. Reich, K. T. Jackson, S. Li, P. Jena and H. M. El-Kaderi, *J. Mater. Chem.*, 2011, **21**, 10629–10632.
28 W. Zhao, S. Han, X. Zhuang, F. Zhang, Y. Mai and X. Feng, *J. Mater. Chem. A*, 2015, **3**, 23352–23359.
29 A. Chrostowska, M. Maciejczyk, A. Dargelos, P. Baylere, L. Weber, V. Werner, D. Eickhoff, H. G. Stammler and B. Neumann, *Organometallics*, 2010, **29**, 5192–5198.
30 S. Hayashi and T. Koizumi, *Polym. Chem.*, 2012, **3**, 613–616.
31 T. Kojima, D. Kumaki, J.-I. Nishida, S. Tokito and Y. Yamashita, *J. Mater. Chem.*, 2011, **21**, 6607–6613.
32 J. Nishida, T. Fujita, Y. Fujisaki, S. Tokito and Y. Yamashita, *J. Mater. Chem.*, 2011, **21**, 16442–16447.
33 A. B. Morgan, J. L. Jurs and J. M. Tour, *J. Appl. Polym. Sci.*, 2000, **76**, 1257–1268.
34 I. G. C. Coutts, H. R. Goldschm and O. C. Musgrave, *J. Chem. Soc. C*, 1970, 488–493.
35 R. J. Doerksen and A. J. Thakkar, *J. Phys. Chem. A*, 1999, **103**, 2141–2151.
36 I. Yamaguchi, T. Tominaga and M. Sato, *Polym. Int.*, 2009, **58**, 17–21.
37 P. I. Paetzold, *Z. Anorg. Allg. Chem.*, 1963, **326**, 64–69.
38 T. Jaschke and M. Jansen, *J. Mater. Chem.*, 2006, **16**, 2792–2799.
39 Z. Kahveci, T. Islamoglu, G. A. Shar, R. Ding and H. M. El-Kaderi, *CrystEngComm*, 2013, **15**, 1524–1527.
40 M. Mastalerz, M. W. Schneider, I. M. Oppel and O. Presly, *Angew. Chem., Int. Ed.*, 2011, **50**, 1046–1051.
41 J. H. Chong, S. J. Ardakani, K. J. Smith and M. J. MacLachlan, *Chem. – Eur. J.*, 2009, **15**, 11824–11828.
42 S. I. Vagin, A. K. Ott, S. D. Hoffmann, D. Lanzinger and B. Rieger, *Chem. – Eur. J.*, 2009, **15**, 5845–5853.
43 C.-F. Chen, *Chem. Commun.*, 2011, **47**, 1674–1688.
44 N. T. Tsui, A. J. Paraskos, L. Torun, T. M. Swager and E. L. Thomas, *Macromolecules*, 2006, **39**, 3350–3358.
45 L. Weber, V. Werner, M. A. Fox, T. B. Marder, S. Schwedler, A. Brockhinke, H. G. Stammler and B. Neumann, *Dalton Trans.*, 2009, 1339–1351, DOI: 10.1039/B815931a.
46 F. Jakle, *Coord. Chem. Rev.*, 2006, **250**, 1107–1121.
47 N. Matsumi, K. Kotera, K. Naka and Y. Chujo, *Macromolecules*, 1998, **31**, 3155–3157.
48 J. An, S. J. Geib and N. L. Rosi, *J. Am. Chem. Soc.*, 2009, **132**, 38–39.
49 B. Li, Y. Duan, D. Luebke and B. Morreale, *Appl. Energy*, 2013, **102**, 1439–1447.
50 H. A. Gasteiger and N. M. Marković, *Science*, 2009, **324**, 48–49.
51 A. Thomas, P. Kuhn, J. Weber, M.-M. Titirici and M. Antonietti, *Macromol. Rapid Commun.*, 2009, **30**, 221–236.
52 M. G. Rabbani and H. M. El-Kaderi, *Chem. Mater.*, 2011, **23**, 1650–1653.
53 P. Mohanty, L. D. Kull and K. Landskron, *Nat. Commun.*, 2011, **2**, 1–6.
54 A. Laybourn, R. Dawson, R. Clowes, J. A. Iggo, A. I. Cooper, Y. Z. Khimyak and D. J. Adams, *Polym. Chem.*, 2012, **3**, 533–537.
55 R. Dawson, A. I. Cooper and D. J. Adams, *Polym. Int.*, 2013, **62**, 345–352.
56 Z. Wang, B. Zhang, H. Yu, L. Sun, C. Jiao and W. Liu, *Chem. Commun.*, 2010, **46**, 7730–7732.
57 O. K. Farha, A. M. Spokoyny, B. G. Hauser, Y.-S. Bae, S. E. Brown, R. Q. Snurr, C. A. Mirkin and J. T. Hupp, *Chem. Mater.*, 2009, **21**, 3033–3035.
58 O. K. Farha, Y.-S. Bae, B. G. Hauser, A. M. Spokoyny, R. Q. Snurr, C. A. Mirkin and J. T. Hupp, *Chem. Commun.*, 2010, **46**, 1056–1058.
59 T. Ben, H. Ren, S. Ma, D. Cao, J. Lan, X. Jing, W. Wang, J. Xu, F. Deng, J. M. Simmons, S. Qiu and G. Zhu, *Angew. Chem., Int. Ed.*, 2009, **48**, 9457–9460.
60 W. Lu, D. Yuan, D. Zhao, C. I. Schilling, O. Plietzsch, T. Muller, S. Bräse, J. Guenther, J. Blümel, R. Krishna, Z. Li and H.-C. Zhou, *Chem. Mater.*, 2010, **22**, 5964–5972.
61 A. P. Katsoulidis and M. G. Kanatzidis, *Chem. Mater.*, 2011, **23**, 1818–1824.
62 T. Islamoglu, T. Kim, Z. Kahveci, O. M. El-Kadri and H. M. El-Kaderi, *J. Phys. Chem. C*, 2016, **120**, 2592–2599.
63 D. Britt, D. Tranchemontagne and O. M. Yaghi, *Proc. Natl. Acad. Sci. U. S. A.*, 2008, **105**, 11623–11627.
64 H. Furukawa and O. M. Yaghi, *J. Am. Chem. Soc.*, 2009, **131**, 8875–8883.
65 C. E. Wilmer, O. K. Farha, Y.-S. Bae, J. T. Hupp and R. Q. Snurr, *Energy Environ. Sci.*, 2012, **5**, 9849–9856.
66 P. Nugent, Y. Belmabkhout, S. D. Burd, A. J. Cairns, R. Luebke, K. Forrest, T. Pham, S. Ma, B. Space, L. Wojtas, M. Eddaoudi and M. J. Zaworotko, *Nature*, 2013, **495**, 80–84.
67 P.-Z. Li and Y. Zhao, *Chem. – Asian J.*, 2013, **8**, 1680–1691.
68 Z. Xiang, X. Zhou, C. Zhou, S. Zhong, X. He, C. Qin and D. Cao, *J. Mater. Chem.*, 2012, **22**, 22663–22669.
69 T. Islamoglu, M. Gulam Rabbani and H. M. El-Kaderi, *J. Mater. Chem. A*, 2013, **1**, 10259–10266.